# The Local Structure of Triphenyl Phosphite Studied Using Spallation Neutron and High-Energy X-ray Diffraction

**Qiang Mei,[†,‡] Prasanna Ghalsasi,[†] Chris J. Benmore,*[,‡] and Jeffery L. Yarger[†]**

*Department of Chemistry, University of Wyoming, Laramie, Wyoming 82071, and I.P.N.S. Division, Argonne National Laboratory, Argonne, Illinois 60439*

*Received: July 21, 2004; In Final Form: September 28, 2004*

Spallation neutron and high-energy X-ray diffraction experiments have been performed to investigate the local structural changes in triphenyl phosphite (TPP) in the crystalline, glacial, glassy, and supercooled liquid phases. The hydrogen/deuterium first-order difference method shows a large increase in intensity due to additional hydrogen correlations in the crystalline spectra compared to the glass and supercooled liquid at ∼3.0 and 3.4 Å. These features are shown to be largely due to inter-phenyl ring H−C/H interactions, which are probably associated in part with the formation of weak intermolecular hydrogen bonds. The high-energy X-ray diffraction data show a decrease in correlations at 3.12 Å which is attributed to changes in C−O/P intramolecular interactions between the glacial and crystalline forms. The structural evolution of the glacial state was also measured over time using total neutron diffraction. The largest structural differences between the early glacial and crystalline states are observed at 3.0 and 4.5 Å. Moreover, as the transformation progresses, the glacial spectra cannot be adequately described as a simple mixture of supercooled liquid and crystalline components. These results suggest that changes in molecular conformation and nearest-neighbor interactions are responsible for the existence of the glacial state.

## Introduction

Kivelson and co-workers have discovered a low-temperature rigid state in the fragile glass former triphenyl phosphite (TPP).[1] It was discovered by annealing the low-temperature glass at 220 K, although it can also be formed by annealing the supercooled liquid. The annealed (high-density) form was initially reported to be amorphous and named the "glacial state". It has been suggested that the TPP molecule may undergo a first-order phase transition from the supercooled liquid to a glassy state of another liquid.[2] However, the nature of the glacial state and existence of a second glassy state is a matter of debate, and alternative interpretations have also been proposed.

Kivelson et al.[3−6] have suggested that the glacial phase is "apparently amorphous" and considered this phase to be a defected-ordered crystal from "frustration-limited cluster formation", a thermodynamic theory of the supercooled liquid.[3,7] The formation of a defect-ordered crystal would be connected to the inability of the system to tile space from the development of a locally preferred structure (i.e., a topological frustration). Therefore, the locally preferred structure (glacial) and ideal crystal structures are expected to be slightly different. In this context, the glacial phase could provide the first experimental evidence of topological frustration in a supercooled liquid, and the investigation of "polyamorphism" of TPP would contribute to the understanding of the supercooled liquid state and the subsequent glass formation.[6]

Conversely, Hedoux et al.[8−14] have performed Raman, neutron, and X-ray diffraction, as well as inelastic neutron scattering experiments, and argue that the glacial state is not amorphous but formed by nanocrystallized domains of the stable crystalline phase, mixed with a fraction of undercooled liquid. The relative fractions of these components depend on the aging temperature. From total neutron diffraction reactor measurements on fully deuterated TPP, Hedoux et al. suggested that the glaciation process can be considered as an aborted crystallization attempt,[8] but no quantitative real-space analysis of the local structure of the liquid or glacial states has yet been reported. Interestingly, crystal structure studies have shown that the TPP molecule does not exhibit an ideal $C_3$ symmetric propeller shape,[15] but one phenyl ring is aligned in the opposite direction (see Figure 1). In addition, Raman spectra have shown that there exist weak C−H···O hydrogen bonds in the glacial state at ∼222−226 K,[9,10,13] which has been used to support the nanocrystalline/supercooled liquid mixture interpretation, because the data can be decomposed into supercooled liquid and crystal contributions.

Small-angle neutron scattering data have observed cluster growth in the glacial state of TPP, which have been interpreted as a four-step model of cluster formation, rapid nucleation, agglomeration, and saturation.[16] However, the reason for saturation still remains elusive. Other possible interpretations have included a highly correlated second liquid,[17] a second glassy form,[2,18] a plastic crystal state,[18,19] or a liquid crystal state.[19] Given the range of explanations describing the glacial state, we have applied the techniques of H/D substitution in spallation neutron diffraction and high-energy X-ray diffraction to obtain a clearer understanding of the structural differences on a local structural scale between the different forms of TPP. Examples of the different types of local interactions which are probed by each technique are illustrated in Figure 1.

* Corresponding author. E-mail: benmore@anl.gov. Phone: 630 252 7665. Fax: 630 252 4163.
[†] University of Wyoming.
[‡] Argonne National Laboratory.

10.1021/jp046762o CCC: $27.50 
Published on Web 12/07/2004

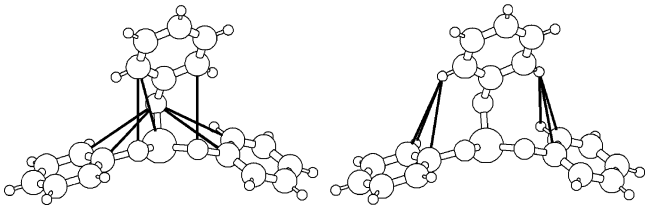

**Figure 1.** Schematic view of the molecular conformation of TPP taken from the X-ray crystal structure. Left: The black lines represent intramolecular heavy-atom interactions (P, O, C) observed in the X-ray measurement between distances of 3.1 and 3.5 Å, namely O−C and P−C correlations. Right: The black lines represent the intramolecular hydrogen interactions C−H and H−H (which dominate the first-order difference neutron signal) between distances of 2.8 and 3.4 Å.

## Experimental Details

Hydrogenated and perdeuterated TPP was obtained by the standard procedure of slowly adding 1 mol of phosphorus trichloride (Aldrich, 97%) to 3 mol of phenol (Fluka) at 60 °C and stirring for 24 h under an inert atmosphere. Purification of the TPP was carried out by fractional distillation under vacuum. The purity of the sample determined by $^{1}$H, $^{13}$C, and $^{31}$P NMR is >99.8%. Differential scanning calorimetry (DSC) was carried out to measure the glass transition temperature of the TPP samples (using a Perkin-Elmer Diamond DSC). The glass transition temperature for both of the samples was determined to be 202 K using a scanning rate of 10 K/min. For H-TPP, the melting temperature is 293.9 K, the glass transition temperature is reported to be 202.9 K, and the crystallization temperature is 237.9 K, according to DSC scans at 0.3 K/min.[12]

High-energy X-ray experiments were made on a hydrogenated TPP sample (the H-TPP purity was greater than 99%) that was sealed in a 4-mm i.d. silica tube and loaded into a helium cryostat. The experiments were performed using an incident beam energy of 115 keV and an angular range of $2\theta = 0.3-20°$, on the 11-ID-C BESSRC beamline at the Advanced Photon Source, Argonne National Laboratory, U.S.A. Hydrogenated TPP samples for high-energy X-ray experiments were measured in the supercooled liquid, glassy, glacial, and crystalline states. Typical uncertainties in the temperatures for this experimental set-up were ∼0.1 K. The glass was measured at 190 K and the crystal at 250 K. The supercooled liquid was measured at 220 K for 2 h. The glacial state was formed by annealing the supercooled liquid, as the transformation is known to occur more slowly than by annealing the glass.[8] Changes in the X-ray structure factor showed that the glacial state was fully formed by annealing the supercooled liquid at 220 K after 4 h, because subsequent data collected for 6 h observed no significant changes in the diffraction pattern.

Neutron scattering experiments were performed at low temperature (190−250 K using a liquid nitrogen cryostat) on a fully deuterated $P(OC_6D_5)_3$ (D-TPP) sample and a 67% fully deuterated, 33% fully hydrogenated mixture $P_{2/3}(OC_6D_5)_2 + P_{1/3}(OC_6H_5)$ sample using the glass, liquid, and amorphous materials diffractometer at Argonne National Laboratory, U.S.A. The TPP samples were loaded into 9.5-mm o.d. (D-TPP) and 6.3-mm (mixture TPP) vanadium cans of 0.1-mm wall thickness in an inert glovebox. Sample temperatures for these experiments were stable to within ∼0.2 K. The 67:33 mixture was chosen to give 15 atom % hydrogen content, balancing the requirements of performing manageable inelastic scattering corrections on a 6.3-mm diameter cylindrical sample, obtaining good statistics in a reasonable period of time (between 2 and 8 h), and providing a measurable isotopic contrast to extract the hydrogen-related interactions. The mixed-isotope sample was made 1−2 days before the neutron experiments were performed and kept at room temperature before cooling. Under these conditions, the sample may undergo a slow interchange esterification, leading to the formation of all of the following species: $P(OC_6D_5)_x(OC_6H_5)_{3-x}$ with $x = 0$, 1, 2, or 3. The consequence of this exchange on the measured spectra is considered in the theory section.

Neutron data was collected on the room-temperature liquid, supercooled liquid at 215 K, and glass at 190 K. For the high-purity D-TPP sample, the glacial phase was formed after annealing the supercooled liquid at 215 K for 2 h. As in the X-ray case, once the glacial state had been formed subsequent data collected for 4 h showed only minimal changes in the diffraction pattern. The small impurity in the isotope mixture TPP liquid sample inhibited the formation of the glacial state. For this sample, the glacial state eventually formed after annealing for 8 h at 218 K. The crystalline spectra were measured at 250 K for D-TPP and at 240 K for the mixture TPP sample.

## Theory and Data Analysis

The quantity measured in a neutron or X-ray diffraction experiment is a differential cross-section, which can be split into two parts. A self-scattering part (relating to Compton and form factors in the X-ray case and inelastic scattering in the neutron case) and a distinct scattering part, $I(Q)$. $I(Q)$ is related to the structure factor $S(Q)$ by

$$S(Q) = \frac{I(Q)}{\left(\sum_{\alpha} c_{\alpha} W_{\alpha}(Q)\right)^2} = \frac{1}{\left(\sum_{\alpha} c_{\alpha} W_{\alpha}(Q)\right)^2} \sum_{\alpha,\beta} c_{\alpha} W_{\alpha}(Q) c_{\beta} W_{\beta}(Q)[S_{\alpha\beta}(Q) - 1] \quad (1)$$

where $c_\alpha$ is the atomic concentration of species α and $W_\alpha$ is the coherent scattering length, $b_\alpha$, for the neutrons[20] and the form factor $f_\alpha(Q)$ for X-rays.[21] $S_{\alpha\beta}(Q)$'s are the Faber−Ziman partial structure factors.[22]

For two isostructural and chemically identical samples, which differ only in their isotopic enrichment of H, interactions pertaining just to the isotopically substituted species can be extracted using the neutron diffraction H/D substitution technique by[23]

$$\Delta S_{\mathrm{H}}(Q) = \frac{I_{\mathrm{D}}(Q) - I_{\mathrm{mix}}(Q)}{\sum_{\alpha}(2-\delta) c_{\alpha} b_{\alpha} c_{\mathrm{H}} \Delta b_{\mathrm{H}}} = \frac{\sum_{\alpha}(2-\delta) c_{\alpha} b_{\alpha} c_{\mathrm{H}} \Delta b_{\mathrm{H}}[S_{\mathrm{HX}}(Q) - 1]}{\sum_{\alpha}(2-\delta) c_{\alpha} b_{\alpha} c_{\mathrm{H}} \Delta b_{\mathrm{H}}} \quad (2)$$

where $\delta = 1$ if $\alpha = \mathrm{H}$ and $\delta = 0$ if $\alpha = \mathrm{P}$, C, or O. The presence of $P(OC_6D_5)_x(OC_6H_5)_{3-x}$ species (with $x = 0$, 1, 2, or 3) in $I_{\mathrm{mix}}(Q)$ is evidence that hydrogen correlations between different phenyl rings of the same molecule will appear in $\Delta S_{\mathrm{H}}(Q)$ in addition to hydrogen correlations between different molecules.

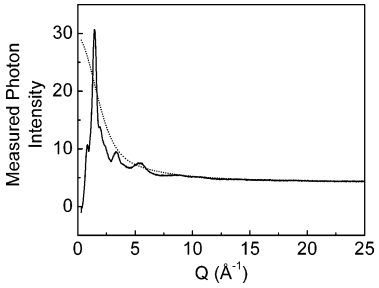


**Figure 2.** Measured high-energy X-ray intensity of the glacial state for the hydrogenated TPP sample (solid line) normalized to the self-scattering plus Compton scattering at high momentum transfers (dotted line).

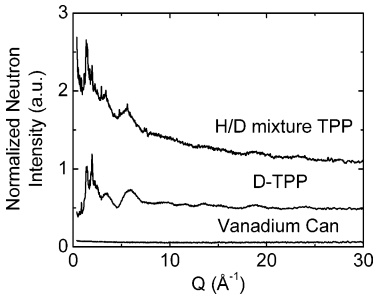


**Figure 3.** Measured neutron intensity of the glacial state for the mixed-isotope TPP sample, fully deuterated TPP, and an empty vanadium can. A few points around 4.05 and 5.05 Å$^{-1}$ have been deleted to eliminate Bragg peaks arising from the vanadium normalization process using raw data.

The differential distribution function $D(r)$ is related to $S(Q)$ via a Fourier transformation

$$D(r) = \frac{2}{\pi}\int_0^{Q\max} Q[S(Q) - 1] \sin(Qr)\, dQ = 4\pi\rho r\cdot[G(r) - 1] \quad (3)$$

where $\rho$ is the atomic number density and $G(r)$ is the radial distribution function. The number density for TPP at 250 K was taken to be 0.0941 (atoms/Å$^{-3}$).[15] An analysis of the high $Q$ level of the $P(OC_6D_5)_3$ diffraction data showed that the change in number density between the supercooled liquid and crystalline samples was less than a few percent, so this number density was used in the data analysis of every low-temperature data set.

In the neutron scattering data analysis, corrections were made for container scattering, attenuation, and multiple scattering and normalized to the scattering from a vanadium rod. This was performed using the *ATLAS*[24] software package for time-of-flight neutron diffraction data. For the X-ray data analysis, corrections were made for detector dead time, container scattering, polarization, and Compton scattering (as shown in Figure 2). The software program *ISOMER-X*[25] was used to reduce the high-energy X-ray diffraction data. At the high X-ray energies used, the X-rays act as a bulk probe, and attenuation and multiple scattering effects were assumed to be negligible.[26] Relativistic corrections were applied at high $Q$ using the Klein Nishina formula.[27] The neutron scattering lengths were obtained from Sears[20] and the atomic form factors and Compton scattering from the tabulated values of Hubbell et al.[21] Figure 3 shows the measured neutron intensity for the glacial state of fully deuterated TPP compared to 67% deuterated TPP and the empty vanadium can. The slope in the mixture sample is due to inelastic scattering effects and was eliminated by fitting the neutron data with a low-order Chebyshev polynomial function

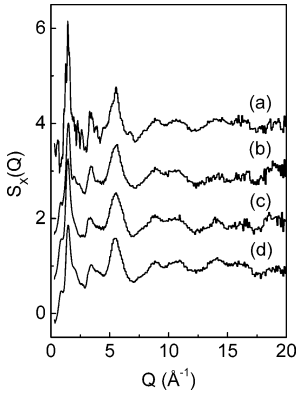


**Figure 4.** Measured high-energy X-ray structure factors for the hydrogenated TPP sample in different forms: (a) crystal at 250 K, (b) glacial state at 220 K, (c) supercooled liquid at 220 K, and (d) glass at 190 K. Curves are offset for clarity.

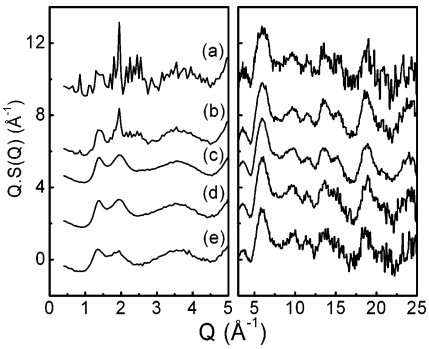


**Figure 5.** Measured total neutron structure factors for the fully deuterated sample in different forms: (a) crystal at 250 K, (b) glacial state at 215 K, (c) supercooled liquid at 215 K, (d) glass at 190 K, and (e) liquid at 298 K. Curves are offset for clarity.

at each angle using the procedure described in the literature.[28] The final total neutron and X-ray $S(Q)$ functions for the supercooled liquid, glass, glacial, and crystalline states are shown in Figures 4 and 5, respectively.

## Results and Discussion

**1. Reciprocal Space.** All of the diffraction measurements were analyzed using a $Q$ spacing of 0.025 Å$^{-1}$. Figure 4 shows the hard X-ray diffraction patterns for the crystal, glacial, supercooled liquid, and glass states of TPP. These spectra are dominated by the heavier atom scattering (i.e., those interactions not involving hydrogen, see Table 1). For the supercooled liquid and glassy spectra, the main low-$Q$ features are a shoulder at 0.84 Å$^{-1}$ and peaks at 1.45 and 3.4 Å$^{-1}$. The main difference between glass or supercooled liquid spectra and the crystal spectra are the growth of small Bragg peaks on these low-$Q$ features. Although the X-ray crystal data shown in Figure 4 suggest that a high degree of disorder is still present in the sample, the positions of the Bragg peaks at low $Q$ are in good agreement with the published crystal structure.[15] This is not the case for the peak intensities, suggesting that there may be some degree of preferred crystallite orientation in the sample. The X-ray structure factor for the glacial state at 220 K shows no clear Bragg peaks, rather the peak observed at 1.45 Å$^{-1}$ in the glass shifts to 1.49 Å$^{-1}$ and the weak shoulder at 1.98 Å$^{-1}$ sharpens. The peak at 0.59 Å$^{-1}$ in the crystal is noticeably absent in the glacial state. However, evidence of Bragg peak formation in the glacial state is observed in the neutron data (shown in Figure 5), suggesting the Bragg peaks may be dominated by hydrogen lattice interactions. This unusual observation also

**TABLE 1: Normalized Faber−Ziman Neutron Weighting Factors for the Measured Total Neutron, $S_N(Q)$, and X-ray Structure, $S_X(Q)$, Factors for $P(OC_6D_5)_3$, as well as the First-Order Neutron Difference Function, $\Delta S_H(Q)$[a]**

| function | P−P | O−O | C−C | H−H | P−O | P−C | P−H | O−C | O−H | C−H |
|---|---|---|---|---|---|---|---|---|---|---|
| X-ray $S_X$ ($Q = 0$) | 0.9 | 2.2 | 44.4 | 0.9 | 2.7 | 12.3 | 1.9 | 19.7 | 2.7 | 12.3 |
| neutron $S_N(Q)$ | 0.1 | 0.5 | 24.4 | 17.1 | 0.3 | 2.1 | 1.7 | 7.1 | 5.9 | 40.8 |
| neutron $\Delta S_H(Q)$ | 0 | 0 | 0 | 34.2 | 0 | 0 | 2.4 | 0 | 8.1 | 55.3 |

[a] The X-ray scattering signal is dominated by the C−C and C−O interactions and the neutron difference by the C−H and H−H interactions.

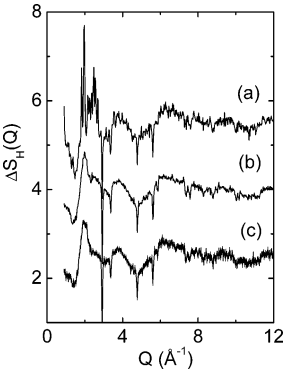


**Figure 6.** First-order difference function neutron structure factors for TPP in different forms: (a) crystal, (b) supercooled liquid, and (c) glass with error bars. The negative dips in the spectra come from 0.17% impurity in the mixture sample (see text). Curves are offset for clarity.

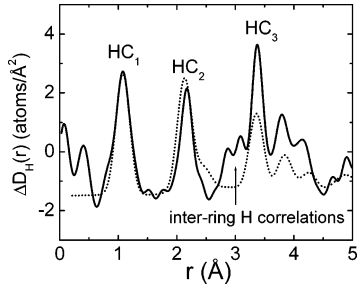


**Figure 7.** Comparison of the measured neutron first-order difference distribution function for the crystal (solid line) with a simple model structure of the intra-phenyl ring hydrogen correlations (dotted line shifted by −1.5; see text). The data and model were both truncated at $Q_{max} = 30$ Å$^{-1}$ and Fourier transformed with a Lorch modification function.

appears to be in agreement with previous findings.[8,11] The principal Bragg peaks are at $Q = 1.96$ Å$^{-1}$ in D-TPP and $Q = 1.97$ Å$^{-1}$ in the mixture TPP sample. Upon cooling, the first peak in the liquid neutron structure factor shifts from $Q = 1.37$ Å$^{-1}$ (298 K) to $Q = 1.39$ Å$^{-1}$ (at 215 K) and is $Q = 1.40$ Å$^{-1}$ in the glass spectra. We note that the positions of the low-$Q$ Bragg peaks in our spectra are only in approximate agreement with the calculated neutron spectra from the published crystal structure[15] (broad overlapping peaks in the neutron data make a quantitative comparison difficult), but the ratios of the intensities of the D-TPP crystal peaks do not agree. The crystal peak intensities also differ from those of previously reported-neutron diffraction results.[8] To check our measurements, the experiment was repeated several times starting from the liquid, but similar intensity ratios were always observed.

The first-order difference (FOD) structure factors for the crystal, glass, and supercooled liquid for TPP are shown in Figure 6. Because the formation of the metastable glacial state occurred at slightly different temperatures and aging conditions in our experiments using two different isotopically labeled samples, this FOD is not shown. Typical error bars for the liquid FOD structure factor are also plotted in Figure 6. All of the features in the FOD curves are associated with hydrogen interactions, except for the sharp dips between $Q = 3-6$ Å$^{-1}$, which arise from the 0.17% crystalline impurity in the mixture TPP sample. Because the impurity peaks are sharp and relatively small and do not change between runs, their presence has a negligible effect on the variations in real-space Fourier transformation of the data. The intramolecular coordination number of carbon around hydrogen of 1.08 Å was used to ensure that the first-order difference structure factor $\Delta S_H(Q)$ was accurately normalized. The Faber−Ziman weighting factors for the FOD are given in Table 1 and show that the scattering for this function is dominated by C−H and H−H interactions, and the O−H weighting is relatively small.

**2. Real-Space Analysis.** To interpret the various peaks in the differential distribution functions, we will first consider the results of the FOD for the crystal (shown in Figure 7), since the structure has been recently refined using a Reitveld analysis.[15] To differentiate between intra- and inter-phenyl ring hydrogen interactions in $\Delta D_H(r)$, a simple model phenyl ring was calculated on the basis of a modified version of the published X-ray crystal structure. It is found that the intra-phenyl ring hydrogen distances H−C$_1$ (hydrogen to the first adjacent carbon atom), H−C$_2$, and H−C$_3$ in the neutron spectra are ∼0.15 Å longer relative to the published X-ray crystal structure data. The bond distances from neutron data are considered to be more accurate and reliable, because neutron scattering is extremely sensitive in probing hydrogen (deuterium) positions.[29] The simple model phenyl ring was constructed from Gaussian peaks in which the C−H bond length was fixed to 1.08 Å, in agreement with the neutron data (see Figure 7). Consequently, the neutron 2.17-Å distance is assigned to H−C$_2$, the 3.37-Å distance to H−C$_3$, and the shoulder at 2.40 Å to intra-ring H−H correlations. The comparison in Figure 7 suggests that the two smaller hydrogen correlation peaks at ∼2.8 and ∼3.0 Å in TPP crystal are most likely due to inter-phenyl (C−H and/or H−H) ring interactions. It is not possible from the isotopic substitutions made in this experiment to ascertain whether these correlations are between phenyl rings in the same molecule or between different molecules. From the modified structural model of the TPP molecule, we find six intramolecular H−C and H−H distances below 3.4 Å (shown in Figure 1) which are very sensitive to the orientation of the phenyl rings, in particular, the inverted ring shown at the top in Figure 1. Two distinct C(H)−O intermolecular hydrogen bond distances at 2.81 and 2.97 Å (between neighboring molecules) have been identified in the crystal structure which lead to H−H and C−H correlations with minimum approach distances of 2.89 and 3.15 Å, respectively. These are illustrated in Figure 8.

Although errors in real space are more difficult to assess than in reciprocal space, long-wavelength systematic errors in $Q$ space are usually manifested as large oscillations at $r < 1$ Å in the unphysical region. Fourier and noise errors generally appear as higher frequency oscillations on the data (e.g., around 1.6 Å in Figure 7). To test the efficacy of the data, Fourier transforms were performed with and without Lorch modification functions at varying values of maximum momentum transfer. It was concluded that the main features in the data reported and

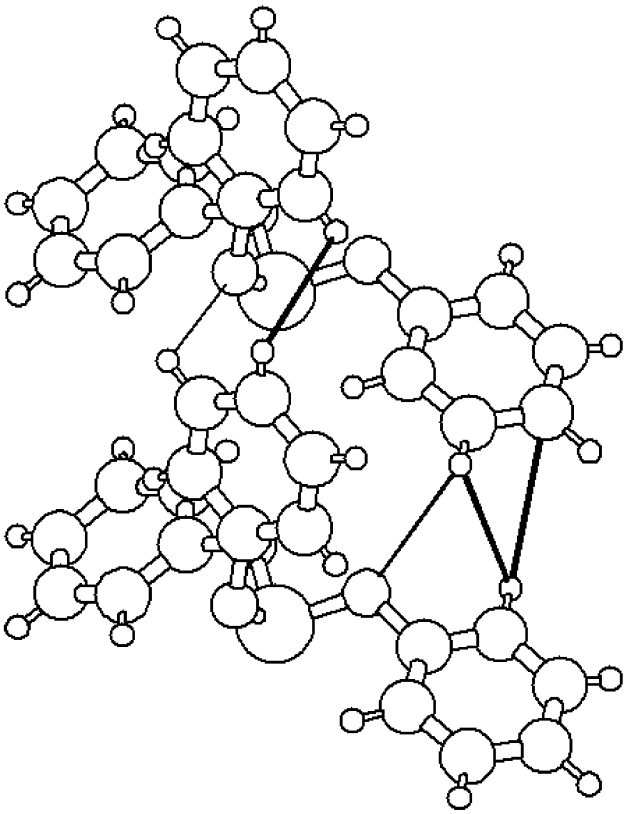

**Figure 8.** Schematic picture of the two shortest H−O intermolecular hydrogen bond distances at 2.81 and 2.97 Å (thin black lines) observed in the X-ray crystal structure and the corresponding shortest intermolecular C−H and H−H distances below 3.15 Å (thick black lines) which dominate the neutron difference function.

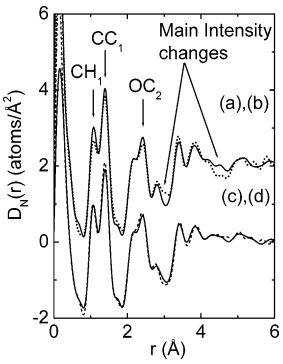


**Figure 9.** Total neutron correlation functions for the fully deuterated sample in different forms corresponding to a Fourier transform of the curves in Figure 5 truncated at $Q_{max} = 25$ Å$^{-1}$ and Lorch function applied. Top: (a) crystal, dotted line; (b) early glacial state at 215 K, solid line (curves offset by +2). Bottom: (c) supercooled liquid, dashed line; (d) glass, solid line.

discussed here appeared to be invariant of the way in which the data were treated.

Next, we consider the non-hydrogen real-space correlations in the total neutron differential correlation function, $D(r)$. The peak at 2.42 Å in Figure 9 is assigned to O−$C_2$ correlations (oxygen to the second adjacent carbon) and the peak at 1.37 Å to overlapping C−C and C−O correlations. The main intensity in the 1.37 Å peak is due to the C−C correlation, as the Faber−Ziman coefficient for the C−C partial structure factor is 3 times larger than that for C−O. As may be expected, the supercooled liquid and glassy neutron $D(r)$ functions look very similar. The main differences between the glacial and supercooled liquid and glassy states are structural changes around 2.8 Å, which are

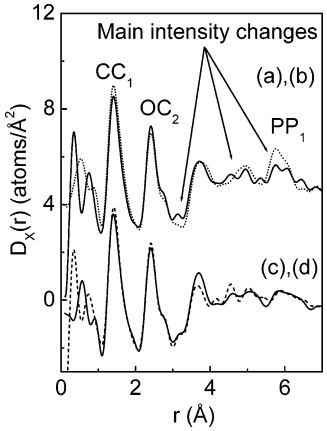


**Figure 10.** Total high-energy X-ray correlation functions for the hydrogenated sample in different forms corresponding to a Fourier transform of the curves in Figure 4 truncated at $Q_{max} = 20$ Å$^{-1}$ and Lorch function applied. Top: (a) crystal, dotted line; (b) glacial state at 220 K, solid line (curves offset by +5). Bottom: (c) supercooled liquid, dashed line; (d) glass, solid line.

much sharper in the glacial form. Larger differences are observed between the crystal and glacial states in the neutron $D(r)$ at 3.0 and 4.5 Å, the latter correlation arising from non-hydrogen-related correlations.

The total X-ray differential correlation functions for TPP in different forms all show a feature at 1.40 Å which arises from C−C and O−C correlations (see Figure 10). This peak shifts from 1.37 Å in neutron diffraction to 1.40 Å in X-ray pattern, because the ratio of the Faber−Ziman weighting factors for these two partials is different in the two cases (see Table 1). The decreased intensity at 3.12 Å in the crystal compared to the other forms is the opposite trend to that observed in the same region of the neutron data. The absence of evidence for significant hydrogen bonding from the Raman results in the liquid[9,10] suggests that this feature is unlikely to be associated with bonding interactions between different molecules at such short distances. Also, because the shortest non-hydrogen intermolecular correlations in the crystal are at 3.27 Å (via the C(H)−O bond), we assign the change in X-ray intensity at 3.12 Å to variations in intramolecular structure between the glacial and crystalline states. This is in agreement with $^{31}$P NMR results.[30] The black lines in Figure 1 (left) show possible carbon atom interactions between 3.1 and 3.5 Å, which may account for the increased intensity at 3.12 Å in the glacial state. Other differences in intensity are observed between crystal and glacial states at 5.74 and 6.04 Å. We note that the crystalline nearest-neighbor P−$P_1$ distance is 5.72 Å.

The FOD differential correlation functions shown in Figure 11 correspond to hydrogen correlations only. The supercooled liquid spectra have a low intensity in the 2.8−3.2 Å region, suggesting few intermolecular C−H or H−H correlations. This agrees with Raman spectroscopy,[9,10] which finds no detectable vibrational bands for the CH−O stretch in the glassy and liquid states. However, it does show two types of weak CH−O hydrogen bonds characterized by two different distances in the crystalline form and that only one of these is present in the glacial state.[13] The formation of these bonds is probably associated with the additional hydrogen peak intensities in the neutron difference function, denoted by the arrows at ∼3.0 and 3.40 Å in Figure 11. To clarify this point, we note that both the crystal and supercooled liquid show features at 3.4 Å in the FOD, which are due in part to intramolecular phenyl ring interactions (see Figure 7). However, these peaks are of considerably different magnitudes in the two spectra, indicating

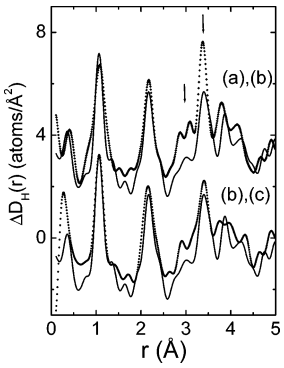


**Figure 11.** Hydrogen-related correlation functions for TPP in different forms, corresponding to the Fourier transforms of the curves in Figure 4 with $Q_{max} = 30$ Å$^{-1}$ and Lorch function applied. (a) crystal, diamonds (offset by +4). (b) supercooled liquid, solid line. (c) glass, circles.

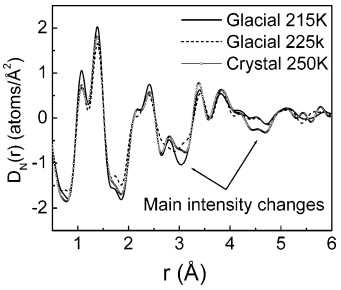


**Figure 12.** Total neutron correlation functions for the fully deuterated sample in the early glacial stage at 215 K, later glacial stage at 225 K, and crystal at 250 K. The data were truncated at $Q_{max} = 25$ Å$^{-1}$.

that additional inter-ring hydrogen correlations must be present in the crystal at 3.4 Å. The glassy spectra show two additional hydrogen-related features: a peak at 2.80 and a shoulder at 3.2 Å, compared to the supercooled liquid. Significant local structural differences are observed between the glass spectra and the supercooled liquid (and crystalline spectra) around 3.8 Å. However, these features require sophisticated modeling techniques to be properly interpreted.

Total neutron correlation functions for the glacial state formed at 215 and 225 K and the crystal at 250 K for the fully deuterated TPP sample are shown in Figure 12. These data show that significant structural rearrangements in the glacial state have to occur in the 2.8−3.0 and 4.5 Å regions before longer-range crystallization can take place. In addition, because the 225 K glacial-state data cannot be simply reproduced by a linear combination of the 215 K glacial state and the crystalline structures, the results suggest that the glacial state is not a simple two-component mixture of the nanocrystalline and supercooled liquid phases. On the basis of the neutron and X-ray results, we suggest that slight variations in molecular conformation as well as changes in the next-nearest-neighbor interactions are responsible for the longer range structural differences between the glacial and crystalline states. Therefore, the glacial state may well originate from a frustration effect caused by competition between optimal molecular conformation (in the glacial form) and weak intermolecular hydrogen bonding effects (in the crystal).

The concept of "locally preferred structure" (LPS) has been proposed by Kivelson and co-workers to interpret the structural changes and the metastable glacial phase.[6,31] A LPS is loosely defined as an arrangement of molecules which, in a given region of the pressure−temperature phase diagram, minimizes some local free energy.[31] It is assumed that there are (at least) two different LPSs in TPP. In the suggested scenario, the first LPS is a TPP molecule cluster which has a low local free energy, because it can assume an optimal molecular conformation. The second type of LPS is a TPP molecule cluster linked by two intermolecular hydrogen bonds, which slightly alters the molecular conformation.

More recently, Tanaka[2] has suggested that the formation of the glacial state has two different mechanisms: nucleation-growth type when $T > 215.5$ K and spinodal-decomposition type when $T < 215.5$ K. From the data presented here and discussion above, our data are consistent with this interpretation but do not provide verification. To address this issue more carefully, we have performed additional time dependence measurements on TPP, to observe the structural evolution of the glacial state using both neutron and high-energy X-ray diffraction techniques. These results and an assessment of changes in molecular conformation in the different forms will be the subject of our future publications.

## Conclusions

Total and hydrogen/deuterium isotopic substitution neutron scattering techniques together with high-energy X-ray diffraction experiments have been performed to investigate the intramolecular and nearest-neighbor interactions for TPP in the crystalline, glacial, glassy, and liquid phases. The combined diffraction data have been used to interpret structural characteristics of the metastable glacial state and investigate the existence of "apparent polyamorphism" in TPP. The neutron results show that the most significant differences in structure between the glacial and crystalline states appear at 3.0 and 4.5 Å. A first-order neutron difference method applied to the crystalline, liquid, and glass data show that hydrogen correlations at distances of 3.0 and 3.4 Å appear only in the crystalline spectra. It is suggested that these features are due to inter-phenyl ring C−H and/or H−H interactions, most probably associated in part with the formation of weak intermolecular hydrogen bonds observed in Raman measurements. The X-ray data show the opposite trend in the same region: namely, a decrease in intensity at 3.12 Å for the crystal compared to the glacial state. This change is attributed to variations in molecular conformation, probably due to C−O/P interactions, between the glacial and crystalline states. It is argued that the glacial state is not a simple mixture of nanocrystalline and supercooled liquid components, but rather, the abortive crystallization attempt arises through competition between the formation weak intermolecular hydrogen bonds and optimum molecular conformation.

**Acknowledgment.** This work was supported by the U.S. Department of Energy (W-31-109-ENG-38), the Department of Defense (ARO-190310143), and the National Science Foundation (CHE-0094202 and CHE-0313661). The authors would like to gratefully acknowledge the help and assistance of Joan Siewenie during data collection on GLAD and Yang Ren for help with the cryostat on 11-ID-C. Jürgen Senker is thanked for providing the TPP crystal structure for modeling.

## References and Notes

(1) Ha, A.; Cohen, I.; Zhao, X.; Lee, M.; Kivelson, D. *J. Phys. Chem.* **1996**, *100*, 1.

(2) Tanaka, H.; Kurita, R.; Mataki, H. *Phys. Rev. Lett.* **2004**, *92*, 25701.

(3) Kivelson, S. A.; Zhao, X.; Kivelson, D.; Fischer, T. M.; Knobler, C. M. *J. Chem. Phys.* **1994**, *101*, 2391.

(4) Kivelson, D.; Kivelson, S. A.; Zhao, X.; Nussinov, Z.; Tarjus, G. *Physica A* **1995**, *219*, 27.

(5) Cohen, I.; Ha, A.; Zhao, X.; Lee, M.; Fischer, T.; Strouse, M. J.; Kivelson, D. *J. Phys. Chem.* **1996**, *100*, 8518.

(6) Kivelson, D.; Tarjus, G. *J. Non-Cryst. Solids* **2002**, *307*−*310*, 630−636.

(7) Alba-Simionesco, C.; Tarjus, G. *Europhys. Lett.* **2000**, *52*, 297.

(8) Hedoux, A.; Dore, J.; Guinet, Y.; Bellissent-Funel, M. C.; Prevost, D.; Descamps, M.; Grandjean, D. *Phys. Chem. Chem. Phys*. **2002**, *4*, 5644−5648.

(9) Guinet, Y.; Denicourt, T.; Hedoux, A.; Descamps, M. *J. Mol. Struct.* **2003**, *651*−*653*, 507.

(10) Hedoux, A.; Guinet, Y.; Descamps, M. *Phys. Rev. B* **1998**, *58*, 31.

(11) Hedoux, A.; Hernandez, O.; Lefebvre, J.; Guinet, Y.; Descamps, M. *Phys. Rev. B* **1999**, *60*, 9390.

(12) Hedoux, A.; Guinet, Y.; Foulon, M.; Descamps, M. *J. Chem. Phys.* **2002**, *116*, 9374.

(13) Derollez, P.; Hernandez, O.; Hedoux, A.; Guinet, Y.; Masson, O.; Lefebvre, J.; Descamps, A. *J. Mol. Struct.* **2004**, *694*, 131−138.

(14) Hedoux, A.; Guinet, Y.; Derollez, P.; Hernandez, O.; Lefort, R.; Descamps, M. *Phys. Chem. Chem. Phys.* **2004**, *6*, 3192−3199.

(15) Senker, J.; Lüdecke, J. *Z. Naturforsch., B* **2001**, *56*, 1089. Hernandez, O.; Hedoux, A.; Lefebvre, J.; Guinet, Y.; Descamps, M.; Papoular, R.; Masson, O. *J. Appl. Cryst.* **2002**, *35*, 212−219.

(16) Schwickert, B. E.; Kline, S. R.; Zimmermann, H.; Lantzky, K. M.; Yarger, J. L. *Phys. Rev. B* **2001**, *64*, 45410.

(17) Muzukami, M.; Kobashi, K.; Hanaya, M.; Oguni, M. *J. Phys. Chem. B* **1999**, *103*, 4078.

(18) Dvinskikh, S.; Benini, G.; Senker, J.; Vogel, M.; Weidersich, J.; Kudlik, A.; Rossler, E. *J. Phys. Chem. B* **1999**, *103*, 1727.

(19) Johari, G. P.; Ferrari, C. *J. Phys. Chem. B* **1997**, *101*, 10191.

(20) Sears, V. F. *Neutron News* **1992**, *3*, 26.

(21) Hubbell, J. H.; Veigele, W. J.; Briggs, E. A.; Howerton, R. J. *J. Phys. Chem. Ref. Data* **1973**, *4*, 471.

(22) Faber, T. E.; Ziman, J. M. *Philos. Mag*. **1964**, *11*, 153.

(23) Benmore, C. J.; Loh, Y. L. *J. Chem. Phys*. **2000**, *112*, 5877.

(24) Soper, A. K.; Howells, W. S.; Hannon, A. C. *Report RAL 89-046*; Rutherford Appleton Laboratory, 1989.

(25) Urquidi, J.; Benmore, C. J.; Neuefeind, J.; Tomberli, B. *J. Appl. Cryst*. **2003**, *36*, 368.

(26) Tomberli, B. L.; Benmore, C. J.; Egelstaff, P. A.; Neuefeind, J.; Honkimaki, V. *J. Phys.: Condens. Matter* **2000**, *12*, 2597−2612.

(27) Klein, O.; Nishina, Y. *Z. Phys.* **1929**, *57*, 853.

(28) Soper, A. K.; Luzar, A. *J. Chem. Phys*. **1992**, *97*, 1320.

(29) Stewart, R. F.; Davidson, E. R.; Simpson, W. T. *J. Chem. Phys.* **1965**, *42*, 3175.

(30) Senker, J.; Rössler, E. *J. Phys. Chem. B* **2002**, *106*, 7592.

(31) Tarjus, G.; Alba-Simionesco, C.; Grousson, M.; Viot, P.; Kivelson, D. *J. Phys.: Condens. Matter* **2003**, *15*, 1077.